BIOCHEMISTRY
including biophysical chemistry & molecular biology
Article

Biochemistry **2010,** *49,* 3965–3976 3965
DOI: 10.1021/bi902090q

Ras-Targeting Action of Thiopurines in the Presence of Reactive Nitrogen Species

Jongyun Heo* and Inpyo Hong

Department of Chemistry and Biochemistry, The University of Texas at Arlington, Arlington, Texas 76019

Received December 6, 2009; Revised Manuscript Received April 5, 2010

ABSTRACT: Thiopurine drugs are commonly used in the treatment of certain cancers, autoimmune disorders, organ transplant rejection, and bowel disease. Because long-term treatment with thiopurines for certain diseases is common, the cytotoxic effects associated with chronic exposure to thiopurine drugs are inevitable. The results shown in this study indicate that the oncogenic Ras in model cancer cell lines forms a complex with thioguanine nucleotide that is derived from long-term treatment with thiopurines. This study also showed that the Ras thioguanine nucleotide binary complex is likely to be a direct target of a redox agent, resulting in downregulation of the oncogenic Ras. This study proposes a radical-based molecular mechanism for the path of Ras-targeting thiopurines used in conjunction with redox agents. Given that Ras plays a central role in cellular signaling pathways, any interference with Ras activity by thiopurines and redox agents has the potential for devastating cytotoxic effects.

Thiopurine drugs such as 6-thioguanine (6-TG), 6-mercaptopurine (6-MP), and azathioprine (AZA) are important chemotherapeutic agents for the treatment of various cancers, including acute myeloid leukemia and adenocarcinomas as well as autoimmune disorders and bowel disease (*1*−*3*). These prodrug thiopurines are also used to prevent organ transplant rejection (*4*−*7*). In cells, the actions of various cellular enzymes convert these treated thiopurines into pharmacologically active 6-deoxythioguanine nucleotide (TdGNP) and 6-thioguanine nucleotide (TGNP) (*1*−*3*, *8*−*10*). TdGNP and TGNP are analogues of deoxyguanine nucleotide (dGNP) and guanine nucleotide (GNP, including both GTP and GDP), respectively; this is because the 6-TG moiety of TdGNP and TGNP shares a structural homology with the guanine base, except that 6-TG has a sulfur atom instead of an oxygen atom at the C_6 position of the guanine base (*11*).

The role of TdGNP in cells has been studied extensively because the immediate and direct primary therapeutic action of thiopurines pertains to the incorporation of TdGNP into DNA as a form of 6-TG that interferes with the action of a mismatch repair system (*12*−*14*). The mismatch repair system recognizes multiple 6-TG incorporations in DNA as a severe DNA lesion, thus inducing programmed cell apoptosis (*7*). Despite the therapeutic benefit of thiopurines, treatment with them has the potential to cause adverse effect(s) because the multiple 6-TGs in DNA can also induce development of methylation tolerance (*15*, *16*).

Recent studies show that redox agents target the sulfur atom of 6-TGs in DNA and thus damage DNA (*7*, *17*, *18*). The redox susceptibility of 6-TGs in DNA is not unusual because the sulfur atoms in biomolecules such as cysteine and glutathione (GSH) are redox sensitive (*19*−*21*). Redox agents include reactive nitrogen species (RNS) and reactive oxygen species (ROS) and mimic the action of GEFs on Ras proteins (*22*−*25*). RNS include nitric oxide (NO), nitrogen dioxide ($^{\bullet}NO_2$), higher oxides (i.e., N_2O_3), and a peroxynitrite ($ONOO^-$) (*26*, *27*). Superoxide anion radical ($O_2^{\bullet-}$), hydroxyl radical ($OH^{\bullet}$), and hydrogen peroxide (H_2O_2) belong to ROS (*26*). Reactions between RNS and/or ROS produce another set of RNS and/or ROS. For example, $ONOO^-$ can be formed by the reaction of NO with $O_2^{\bullet-}$ (*28*). This $ONOO^-$ is known to be a powerful and destructive oxidant (*29*, *30*), an effect most likely owed to its high reduction potential (*31*). $ONOO^-$ can be decomposed into $^{\bullet}NO_2$ and a small fraction of $OH^{\bullet}$ (*28*). $ONOO^-$ can also react with CO_2 to produce $^{\bullet}NO_2$ and a carbonate radical ($CO_3^{\bullet-}$) (*32*).

Unlike the situation with TdGNP, few studies have been made of the action and fate of TGNP in cells. Studies show that small GTPases, such as the proto-oncoprotein $p21^{Ras}$ (Ras), can bind with TGNP (*8*, *33*). This is not unusual because TGNP is an analogue of GNP that is a ligand of small GTPases (*vide supra*). Ras GTPases function by cycling between inactive GDP-bound and active GTP-bound states (*34*, *35*). This cycling is controlled by various regulators, such as GTPase-activating proteins (GAPs) and guanine nucleotide exchange factors (GEFs) (*34*, *35*). GAPs downregulate GTPase activity by stimulating the intrinsically slow rate of GTP hydrolysis to populate GTPase in its inactive GDP-bound form; in contrast, GEFs upregulate GTPase functions by promoting guanine nucleotide exchange (GNE) to generate the active GTP-bound state of GTPase *in vivo* (*36*−*44*). Studies show that certain RNS and ROS mimic the action of GEFs on Ras proteins. The reaction of the redox-sensitive Ras Cys^{118} side chain with $^{\bullet}NO_2$ produces a thiyl radical that mechanically initiates facilitation of nucleotide dissociation from Ras proteins (*22*, *23*, *25*). If NO is present in addition to $^{\bullet}NO_2$, the $^{\bullet}NO_2$-mediated nucleotide dissociation process can be coupled with formation of a redox-inactive S-nitrosated Ras (Ras-SNO) (*25*). However, this radical-based S-nitrosation process may not be applicable for other cellular proteins because an O_2-independent transnitration is suspected of dominating protein S-nitrosations in cells (*45*). Unlike the S-nitrosation process, the molecular mechanism(s) by which the Ras Cys^{118} side chain is oxidized into forms of sulfenic, sulfinic, and sulfonic acid remain(s) undefined.

As noted elsewhere, the 6-TG sulfur atom in DNA is redox sensitive. Hence, the question arises of whether RNS target the sulfur atom of TGNP when it is bound to Ras. If so, do RNS

*Corresponding author. E-mail: jheo@uta.edu. Telephone: (817) 272-1076. Fax: (817) 272-3808.

© 2010 American Chemical Society
Published on Web 04/08/2010

perturb Ras activity cycling by targeting the Ras-bound TGNP? What is the effect of TGNP in combination with RNS on the Ras-mediated cellular signaling effect? This study, using Ras-activated cancer cell lines, has examined, with and without the presence of RNS, the cellular effect associated with the perturbation of Ras activity as a consequence of treatment with thiopurines.

This study also characterizes the fundamental biochemical properties of Ras with TGNP in combination with GNP *in vitro*. The results of this study further suggest that a molecular mechanism underlies the combined action of thiopurines and redox agents on regulation of Ras activity. Moreover, the results and analyses shown in this study promote a better understanding of the potential cytotoxicity associated with the Ras-targeting action of thiopurines under oxidative stress conditions (i.e., induced by cellular RNS and/or ROS).

MATERIALS AND METHODS

Cell Culture. Bladder carcinoma (T24) and fibrosarcoma (HT1080) cell lines were obtained from the American Type Culture Collection (Manassas, MD) and cultured in Dulbecco's modified Eagle medium supplemented with 10% fetal bovine serum (DMEM/fetal bovine serum).

Cell Treatments. Given that the tumor cell lines used in this study were unable to survive under anaerobic conditions (an inert N_2 gas atmosphere, $O_2 < 3$ ppm) for > 1 h, aerobic experimental conditions for cells used in this study were inevitable. However, this led to another problem: Because in the presence of O_2 NO is converted into other RNS (*26*, *27*), a cell culture treated with an NO donor under aerobic conditions results in cells being poised with various RNS. Consequently, it was impossible to discern and identify cellularly active RNS on the basis of this cell study's results. Therefore, cellularly active Ras-targeting RNS was deduced from a comparison of the results of this cell study with *in vitro* kinetic studies. The cell experiments began by treating the cells with a NO-releasing agent *S*-nitrosoglutathione (GSNO) or diethylenetriamine/nitric oxide (DETA/NO) under an aerobic atmosphere. Afterward, the samples were treated repeatedly with the NO donor to continue the effect of RNS on cells. Because the half-life of GSNO and DETA/NO is ~8 and ~20 h, respectively, at pH 7.4 and 37 °C (*46*−*48*), their treatment intervals were 8 and 20 h to ensure the concentration of NO remained for the duration of the experiment at a minimal 50% of the initial concentration of NO in the culture media. DETA/NO was decomposed by leaving the DETA/NO solution for 3 days at room temperature; this decomposed DETA/NO was used as a control for the DETA/NO treatment. Similar to the procedure used in the NO donor treatment, once cells were poised with 6-TG or an apoptotic inducer, they were continuously treated with 6-TG or an apoptotic inducer, respectively, every 48 or 24 h, unless otherwise noted.

Cytotoxicity Assays. A cell viability assay employing 3-(4,5-dimethylthiazol-2-yl)-2,5-diphenyltetrazolium bromide (MTT) was performed to assess the cellular effect of a NO donor in the presence or absence of 6-TG, as described in previous studies (*49*, *50*). The apoptotic effect of a NO donor and/or 6-TG or an apoptotic inducer on cells was measured using the ApoAlert Caspase-3/8 colorimetric assay kit (Takara, Japan). A soft agar-based clonogenic assay also was performed to examine an anchorage-independent growth of tumor cells in the presence and absence of a NO donor and/or 6-TG, as described in previous studies (*51*, *52*).

Determination of Content of Active Ras in Cells. Various buffers were used for the Western analysis of the tumor cell samples treated with a NO donor and/or 6-TG. The extraction buffer consisted of 50 mM NaCl, 5 mM $MgCl_2$, 1 mM ethylenediaminetetraacetic acid (EDTA), 0.1 mM diethylenetriaminepentaacetic acid (DTPA), and 0.1% NP40 in 150 mM Tris-HCl (pH 8.0). The sample buffer contained 50 mM NaCl, 5 mM $MgCl_2$, 10% glycerol, 300 mM β-mercaptoethanol, 1 mM EDTA, 0.1 mM DTPA, and 2% SDS in 50 mM Tris-HCl (pH 7.0). The preparation buffer was composed of 0.1 mM $MgCl_2$, 1 mM EDTA, and 0.1 mM DTPA in 1 mM $(NH_4)_2CO_3$ (pH 7.0). The presence of cellularly active Ras GTPases, including HRas, KRas, and NRas, during the course of the cell experiments was monitored using an immunoblotting analysis that uses an anti-pan-Ras monoclonal antibody (EMD Biosciences). Total cell lysates in the extraction buffer were nutated with glutathione−Sepharose beads coupled with the glutathione *S*-transferase fused with Ras-binding domain (GST-RBD) of Raf1 (residues 51−131) at 4 °C for 1 h, as described in the previous study (*53*). Beads were collected by centrifugation and then washed three times with the extraction buffer. Proteins bound to beads were eluted with the sample buffer. Eluents were electrophoresed, blotted onto a nitrocellulose membrane, and then probed with the anti-pan-Ras monoclonal antibody in conjunction with a secondary antibody conjugated with alkaline phosphatase (Promega).

To examine the quantity of active HRas in T24 cells treated with a NO donor and/or 6-TG, the immunoblotting analysis performed for monitoring generic cellular Ras activities (*vide supra*) was repeated with an antibody specific for HRas (F235) (Santa Cruz Biotechnology). Total HRas expression (active plus inactive HRas) was also determined by a Western blotting analysis using the anti-HRas antibody (F235). Cell lysates in the extraction buffer were electrophoresed and blotted on a nitrocellulose membrane before being probed with the anti-HRas antibody (F235) in combination with a secondary antibody conjugated with alkaline phosphatase.

Raf-1 Kinase Activity Assay. Total cell lysates in the extraction buffer were nutated with glutathione−Sepharose beads conjugated with an anti-Raf-1 antibody (Sigma-Aldrich) at 4 °C for 2 h. The beads thus collected were washed, and the proteins bound to beads were eluted with the sample buffer. Total Raf-1 expression was then determined by a Western blotting analysis using the anti-Raf-1 antibody coupled to glutathione−agarose beads (Pierce). Kinetic assays were performed with catalytically inactive glutathione *S*-transferase-MAP kinase1 (GST-MEK1; Stratagene) as a substrate (0.3 μg/100 μL) at room temperature for 30 min in an assay buffer containing 10 mM $MgCl_2$, 0.1% 2-mercaptoethanol, 100 mM NaCl, 20 μM ATP, 10 μCi of [γ-^{32}P]ATP, and 50 mM Tris-HCl (pH 7.5). The reaction was terminated by boiling the assay mixture for 5 min. This heat-treated sample was then subjected to electrophoresis, blotted on a nitrocellulose membrane, and subsequently analyzed with a PhosphoImager.

Identification of Ras-Bound Nucleotides and Ras S-Nitrosation by Using Mass Spectrometric Analyses. Cell lysates in the extraction buffer were incubated with the anti-pan-Ras monoclonal antibody or the anti-HRas antibody precoupled to glutathione−agarose beads. The beads were isolated by centrifugation and washed three times with the extraction buffer. Ras proteins on beads were then eluded with the preparation buffer and lyophilized using a speed vacuum. The protein samples were then resuspended in a mixture of 40% methanol and 60% in the sample buffer, which also contained 0.1% formic acid (final concentrations). In the next step, the samples were filtered with

Amicon Centricon (10 kDa cutoff) and subjected to brief centrifugation to separate Ras-released nucleotide ligands from the denatured Ras portion. The filtered nonprotein liquid fraction was subjected to an electrospray ionization−mass spectrometry (ESI-MS) and tandem mass spectrometry (MS/MS) analyses so as to characterize the Ras-released ligands. The precipitant protein portion was resuspended in the preparation buffer, digested with trypsin for 10 h, and analyzed with matrix-assisted laser desorption/ionization-time of flight (MALDI-TOF) tandem mass spectrometry. In all mass spectrometry analyses, only singly charged peptides and ions ($[mass + H]^+$) were observed. Thus, the molecular masses determined by these mass spectrometry analyses are 1 Da higher than the molecular masses for the same chemicals at a neutral pH (i.e., pH 7.5).

Ras Protein Sample Preparations. For convenience, HRas and its mutant proteins were used exclusively for all *in vitro* kinetic analysis. The structural architecture of the redox components of HRas, such as the NKCD motif and the Phe^{28} side chain associated with the bound nucleotide, is the same as those of N and KRas. Therefore, the kinetic properties determined for HRas that are associated with redox chemistry can be directly applicable to other Ras isomers, NRas and KRas. Ras proteins, including wild-type (wt) Ras(1−166) and its mutant forms G12V and Q61K, were expressed in and purified from *Escherichia coli* as described previously (*54*, *55*).

To produce a redox-inactive form of wt Ras protein, the purified wt Ras protein was S-nitrosated with NO gas in the presence of O_2 (*22*, *27*). The content of Ras-SNO was measured using the Saville assay (*56*) as described in the previous study (*27*). The maximal mole fraction of the Ras-SNO moiety per total mole of Ras protein was ~0.64 ([Ras-SNO]/[total Ras] = ~0.64). The $^{\bullet}NO_2$-mediated nucleotide dissociation from the Ras-SNO sample was minimal, indicating that the non-Ras-SNO fraction (~0.36) in the Ras sample was redox inactive. It was shown that a significant fraction of the Ras Cys^{118} side chain of Ras samples expressed in and purified from *E. coli* was in redox-inactive oxidized states such as sulfenic acid, sulfinate, and sulfonate (*25*). The presence in the Ras S-nitrosation sample of a fraction of the redox-inactive oxidized forms of Ras was not a problem for the purposes of the experiment. This is because the S-nitrosated Ras was only produced with the objective of producing redox-inactive Ras proteins and thus was incidental to the experiments. Nucleotide-deficient Ras proteins were prepared according to the previous protocol (*57*, *58*). Ras GTPase bound with TGDP, TGTP, or fluorescent 2′- (or 3′-) *O*-(*N*-methylanthraniloyl)-guanosine 5′-diphosphate-attached GDP (mantGDP) was prepared by incubation of the nucleotide-free Ras with TGDP, TGTP, or mantGDP, respectively, as described in previous studies (*57*, *58*).

Kinetic Experimental Conditions. To remove these transition metals from the kinetic assay buffer, 50 mM Tris-HCl (pH 7.5) was passed through a metal-chelating column (Bio-Rad Chelex-100 cation exchange) before adding the highest grade of 50 mM NaCl, 5 mM $MgCl_2$, 1 mM EDTA, and 0.1 mM DTPA. All protein samples (e.g., purified Ras) were dialyzed with a metal-free buffer under anaerobic conditions before performance of any of the assays. Vials for the assays were soaked with 1 N HCl for 1 day and then rinsed with doubly distilled water. A typical redox agent-mediated Ras guanine nucleotide exchange (GNE) assay uses radiolabeled nucleotides (*23*, *25*). However, because radiolabeled TGNP was unavailable at this time, a phosphate assay employing malachite green (*59*) was used to determine the quantity of nucleotide (GDP, TGDP, or TGTP) released from Ras in the course of treatment with redox agents. Inorganic phosphate (NaH_2PO_4) was used as a standard for the phosphate assay. This phosphate assay also was used to determine the intrinsic rate of Ras GTPase activity for TGTP by detecting Ras-released free phosphate over time. Fluorescence mantGDP was substituted for GDP as a way to monitor the competition between GDP and TGDP for a site where one or the other could bind with Ras. This substitution was necessary because normal GDP and TGDP cannot be monitored under our experimental methods.

Determination of the Binding Interaction between Ras and TGDP. Nucleotide-free Ras protein (1 μM) in 400 mM $(NH_4)_2SO_4$ was transferred to a vial (1 mL) containing various concentrations of TGDP (0−50 μM) in the assay buffer and incubated for 1 min at 25 °C. An aliquot of the Ras TGDP mixture was then spotted onto a nitrocellulose membrane. The membrane-bound Ras protein was treated with 500 mM $(NH_4)_2SO_4$ for 1 h and was respotted onto a nitrocellulose membrane to separate the freed TGDP. The quantity of the freed TGDP in the filtered liquid fractions was then analyzed with a phosphate assay (*59*). Nucleotide-free Ras protein without treatment with TGDP was used as a background, and the background value was subtracted from all phosphate assay values determined for the Ras TGDP titration. Because TGDP contains two phosphates, the estimated mole of the freed TGDP corresponding to the Ras-bound TGDP was divided by 2. The values obtained were converted into the mole fractions of bound TGDP per moles of Ras GTPase and plotted against the TGDP concentration.

Determination of the Competitive Binding Interaction of TGDP with mantGDP for Ras. Nucleotide-free Ras protein (1 μM) in 400 mM $(NH_4)_2SO_4$ was transferred to a vial (1 mL) containing various concentrations of TGDP (0−20 μM) in the assay buffer in the presence of a fixed concentration of mantGDP (2.5 μM) at 25 °C. A fluorometer was then used to determine the competitive pseudo-first-order association rates of mantGDP with Ras as a change in the mant fluorescence intensity over time (*57*).

Determination of the Ras GTPase Activity for TGDP. TGTP-bound Ras GTPase (1 μM) was placed in the assay buffer (1 mL) at 25 °C. An aliquot of the sample was withdrawn at the appropriate intervals and spotted onto a nitrocellulose membrane. The quantity of free phosphate (P_i) in the filtered liquid fractions was then analyzed with a phosphate assay (*59*). The phosphate assay values were converted into a fraction of P_i released per TGTP-bound Ras GTPase and plotted over time. Note that, under these experimental conditions, not only P_i but also nucleotides such as GDP, TGDP, GTP, and TGTP can be released from Ras. However, the phosphate analysis used here cannot distinguish between free P_i and phosphates in nucleotides. An ESI-MS analysis of the sample used for the phosphate assay showed that mass peaks corresponding to nucleotides were insignificant but a mass peak for P_i is dominant (not shown). Therefore, the results of the phosphate analysis represent the quantity of P_i released from Ras over time.

Determination of the Effect of RNS on the Ras Interaction with TGDP. The target action of each RNS on Ras GTPases associated with TGNP was specified in kinetic studies performed under anaerobic experimental conditions. Anaerobic kinetic experimental conditions were achieved by using an anaerobic vacuum manifold system in which O_2 was removed by applying a vacuum to airtight serum stoppered-sealed assay vials and followed by filling the vials with an inert gas, N_2, as described in a previous study (*27*).

The cellularly relevant RNS examined in this kinetic study include purified authentic NO and NO_2 gases as well as N_2O_3 (a 1:1 stoichiometric mixture of NO and NO_2 (v/v)) (*22*, *25*, *27*). The amounts of NO and $^{\bullet}NO_2$, respectively, in the assay vials were measured by using a hemoglobin assay and NO_2^-/NO_3^- assay kit-C II (Dojindo) under anaerobic conditions (*24*, *27*). The state of N_2O_3 is dynamic because it can be degraded into NO and $^{\bullet}NO_2$, which then can react to re-form N_2O_3 (*26*). Therefore, the exact concentration of N_2O_3 in an assay solution cannot be determined. The initial concentration of NO in the mixture of NO and $^{\bullet}NO_2$ to produce N_2O_3 was used to express the N_2O_3 concentration. Given that transition metals form a complex with NO to produce metal nitrosyls (*60*), the removal of transition metals was essential to examine the precise action of NO on Ras with TGDP.

GDP- or TGDP-bound Ras (1 μM) was placed in the assay vial (1 mL) containing the kinetic assay buffer. The reaction was initiated by addition of a redox agent (e.g., NO, $^{\bullet}NO_2$, or N_2O_3, ~3 μM each) under anaerobic conditions, and sample aliquots were subtracted from the assay vial at specific intervals, quenched with ascorbic acid, and spotted onto nitrocellulose filters; the phosphate content in the filtered liquid fractions was determined colorimetrically by using a phosphate assay (*59*). The values thus obtained were converted into the mole fractions of nucleotide per moles of total Ras GTPase proteins. Because GDP contains two phosphates, the estimated mole fraction ratio between nucleotides and GTPases was halved. Ras nucleotide dissociation rates were then estimated by using Prism software to fit the result to a one-phase exponential decay.

RESULTS

Effects of Thiopurines on Ras-Activated Bladder Carcinoma and Fibrosarcoma Cells. Studies show that the presence of a Ras variant, G12V, gives T24 cells their malignant property (*61*−*64*). When T24 cells were poised with 6-TG (1 μM), cell viability declined drastically within 24 h (Figure 1A). Furthermore, the slow rate of the anchorage-independent growth of T24 cells in the presence of 6-TG indicates that 6-TG inhibits the growth of cancerous T24 cells (Figure 2B). Similar results were also observed when other thioguanine analogues such as 6-MP and AZA were used instead of 6-TG (not shown). Moreover, the results are reproducible with other cancer cells such as HT1080 cells that have the constitutively active Q61K Ras (not shown). As the previous studies found (*65*−*69*), the immediate apoptotic responses of these tumor cells to treatment with thiopurine drugs are likely caused by the incorporation of a cluster of multiple 6-TGs into DNA. This incorporation initiates programmed cell death by the MMR system.

Some cells (~20% of the initial cells) that survived their initial treatment with 6-TG (1 μM) resisted additional treatment with 6-TG (1 μM for every 48 h) and even slowly regrew in the presence of 6-TG (Figure 1A). Similar results have been observed previously and attributed to the development in cells of thiopurine-mediated methylation tolerance (*15*, *16*). This resistance could be a problem in the long term use of thiopurines to treat patients; this is because chronic exposure to thiopurine drugs often leads to resistance that decreases the drug's effectiveness (*70*−*72*).

Effects of RNS on Ras-Activated Bladder Carcinoma and Fibrosarcoma Cells. Treatment with the NO-releasing agent GSNO or DETA/NO (1 mM) decreases the viability of Ras-activated bladder carcinoma and fibrosarcoma cells (Figure 1A). The effect of decomposed DETA/NO was minor (not shown).

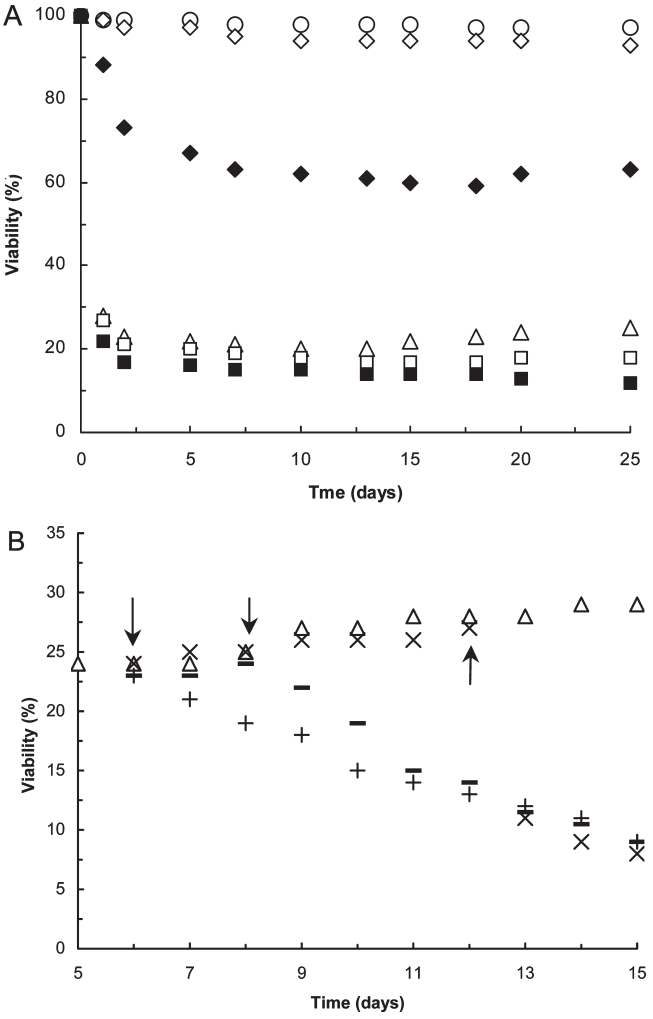

FIGURE 1: Effect of 6-TG and/or GSNO on viability of T24 cells. (A) T24 cells (~2×10^4) were poised with 6-TG and/or GSNO for 25 days as described in Materials and Methods: control (no treatment) (○); GSNO (10 μM) (◇); GSNO (1 mM) (◆); 6-TG (1 μM) (△); 6-TG (1 μM) plus GSNO (10 μM) (□); 6-TG (1 μM) plus GSNO (1 mM) (■). (B) T24 cells (~2×10^4) were initially treated with 6-TG (1 μM), followed by addition of GSNO (10 μM) on days 6 (+), 8 (−), and 12 (×) as indicated by arrows. Cells treated only with 6-TG (1 μM) are shown as a control (△). MTT cell viability assays were performed at the indicated times, as described in Materials and Methods, to assess the effects of 6-TG and/or GSNO.

However, when the concentrations of treated GSNO or DETA/NO were less than 10 μM (e.g., in a range between 2 and 10 μM), the viability of these tumor cells was unaffected (Figure 1A).

The MALDI-TOF analysis for the immunoprecipitated Ras in the GSNO-treated T24 and HT1080 cells indicates that the majority of Ras GTPases in these cells was in the form of Ras-SNO (Figure 2). Formation of Ras-SNO through treatment with NO-releasing agents was observed in previous studies (*73*, *74*).

Taken together, these results suggest that in the presence of NO under aerobic conditions the oncogenic Ras in these tumor cells was converted into a Ras-SNO form. However, formation of Ras-SNO did not interfere with the activity status of this oncogenic Ras and had no effect on the property of these cells.

Effect of Thiopurines on Ras-Activated Bladder Carcinoma and Fibrosarcoma Cells in the Presence of RNS. No noticeable changes occurred in the viability or in the death and growth rates of thiopurine-resistant cells treated for $< \sim 7$ days with 6-TG (1 μM) in the presence GSNO or DETA/NO (10 μM)

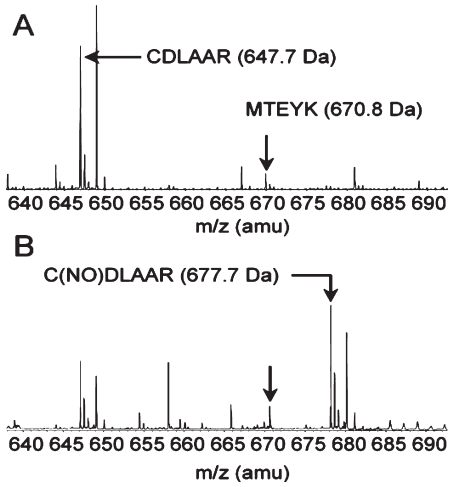

FIGURE 2: Mass spectrometry determination of Ras S-nitrosation in GSNO-treated tumor cells using MALDI-TOF analysis. T24 cells were treated with 6-TG (1 μM) or GSNO (10 μM) for 15 days. The presence of active Ras GTPases (including HRas, NRas, and KRas) per cell mass ($\sim 2 \times 10^6$) was determined using immunoblotting analyses as described in Materials and Methods. A trypsin-digested Ras protein sample was prepared from T24 cells nontreated (A) and treated (B) with GSNO (10 μM) for 15 days and was analyzed with MALDI-TOF as described in Materials and Methods. The mass peak at 647.7 Da represents Ras trypsin-digested peptide C^{118}DLAAR, and the peak at 677.7 Da matches the S-nitrosated C^{118}DLAAR (C^{118}(NO)LAAR) of the fragment. (A) and (B), respectively, denote any of the Ras samples taken from cell culture time points a day before and a day after continuous treatment with GSNO (10 μM) for 10 days.

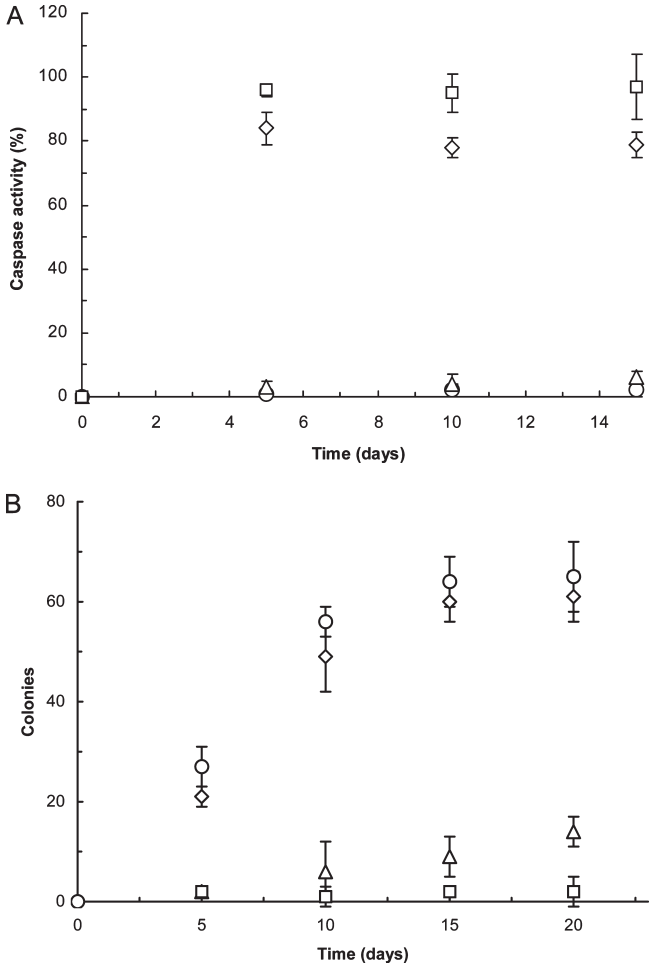

FIGURE 3: Effects of 6-TG and/or DETA/NO on caspase-3/8 activities in T24 cells and on anchorage-independent growth of T24 cells. (A) T24 cells ($\sim 1 \times 10^6$) cultured in a 96-well culture plate were treated with 6-TG and/or DETA/NO for 15 days: control (no treatment) (○); DETA/NO (10 μM) (△); 6-TG (1 μM) (◇); 6-TG (1 μM) plus DETA/NO (10 μM) (□). Apoptotic inducers, 2-amino-*N*-quinolin-8-ylbenzenesulfonamide (10 μM) and 17-(allylamino)-17-demethoxygeldanamycin (2 μM), were used as positive controls. The caspase-3/8 activities of these T24 cells were measured colorimetrically as described in Materials and Methods. The determined values of caspase-3/8 activities were normalized with the mean value of the positive controls (set at 100%). (B) Dishes (six wells) were layered with 0.4% agar in DMEM/fetal bovine serum for soft agar assays. This basal layer was overlaid with a second layer of 2 mL of 0.3% agar in DMEM/fetal bovine serum containing a suspension of $\sim 2 \times 10^3$ cells. The upper agar layer was then overlaid with 1 mL of DMEM/fetal bovine serum with or without addition of 6-TG and/or DETA/NO: control (no treatment) (○); DETA/NO (10 μM) (◇); 6-TG (1 μM) (△); 6-TG (1 μM) plus DETA/NO (10 μM) (□). The cultures were incubated for more than 20 days at 37 °C, and the number of colonies with diameters greater than 0.2 mm was counted on the dates indicated. Results for both (A) and (B) are expressed as an average of three independent experiments; the vertical bar represents standard errors.

(Figures 1B and Figure 3). However, cell viability began to decline when thiopurine-resistant cells were incubated for $> \sim 10$ days with 6-TG (1 μM) in the presence GSNO or DETA/NO (10 μM) (Figure 1B). The decline in tumor cell viability was linked with apoptosis (Figure 3A) and a slow anchorage-independent growth rate (Figure 3B). Also, a significant amount of HRas in T24 cells was rendered inactive under these conditions (Figure 4A). The activity of Raf-1, one of the Ras downstream effectors, also declined when thiopurine-resistant cells were incubated for $> \sim 10$ days with 6-TG (1 μM for every 48 h) and GSNO (or DETA/NO, 10 μM) (Figure 4B). Notice that most of the Ras protein is in the form of Ras-SNO when cells are treated continuously with a NO releasing agent (Figure 2). The results suggest that, in thiopurine-resistant cells, a redox agent(s) downregulates redox-inactive Ras-SNO and thus its downstream signaling protein Raf-1.

Analysis of Ras-Bound Nucleotides from Ras-Activated Tumor Cells Treated with Thiopurine and/or Redox Agents. By using Ras as a probe, TGNP could be detected in T24 cells treated with 6-TG (1 μM for every 48 h) for $> \sim 10$ days (Figure 5A). The result suggests that thiopurine drugs, as a form of TGNP, target Ras in T24 cells. This occurs much slower, however, than the action of thiopurines in targeting DNA as a form of TdGNP.

In order to assess the molecular and cellular status of TGNP associated with Ras in the presence of RNS, Ras was isolated from T24 or HT1080 cells that had been continuously treated for 15 days with thiopurine drugs in the presence of GSNO. The Ras-bound nucleotides were extracted by treatment with denaturing agents (methanol and formic acid) in the sample buffer. The molecular mass of the major species of the Ras-released nucleotides in the presence of RNS was determined to be 463.3 Da (Figure 5B,C). The mass matches that of 5-guanidino-4-nitroimidazole diphosphate (NIm-DP) (*22*). MS/MS analysis also supports a finding that the 463.3 Da peak corresponds to NIm-DP (Figure 6).

NIm-DP was detected when Ras activity was deregulated, and the growth of these cells came to a stop after treatment with both 6-TG and GSNO (or DETA/NO, 10 μM) (Figure 3A). These events suggest that Ras activity and the halt to the tumorous growth of these cells are linked to formation of NIm-DP or *vice versa*.

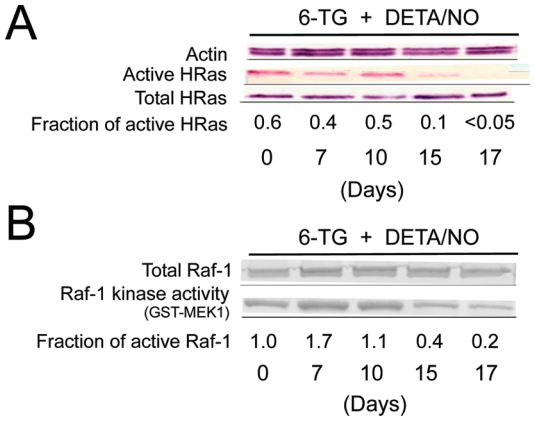

FIGURE 4: Examination of Ras activity in T24 cells treated with various reagents. (A) T24 cells were treated with 6-TG (1 μM) and DETA/NO (10 μM) for 17 days. The presence of active and total HRas (per $\sim 2 \times 10^5$ cells) was probed using immunoblotting analyses as described in Materials and Methods. Optical density quantifications for the active and total HRas bands were performed with a densitometer. The presence of active HRas per total HRas was expressed as a fraction ([active HRas]/[total HRas]). Standard errors are less than 30% of the value shown. (B) Identical cells used for HRas activity analysis (panel A) were analyzed for Raf-1 kinase activity. Cell lysates were subjected to co-IP with an anti-Raf-1 antibody, and total Raf-1 and Raf-1 kinase activity was analyzed as described in Materials and Methods. The fraction of normalized Raf-1 indicates the densitometric ratio of total Raf-1 expression to active Raf-1. Standard errors are less than 30% of the value shown. Actin expression in cells was used as a control for all experiments.

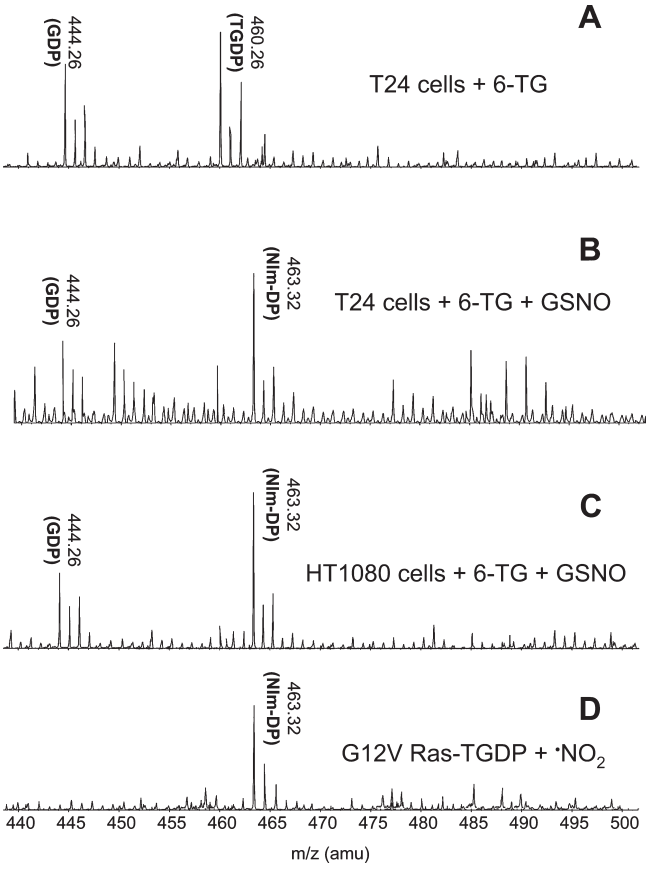

FIGURE 5: Determination by ESI-MS of the molecular weight of the RNS-mediated Ras-bound TGNP dissociation product. (A) T24 cells ($\sim 2 \times 10^4$) were treated with 6-TG (1 μM) for 15 days. (B) T24 cells ($\sim 2 \times 10^4$) were treated with 6-TG (1 μM) in the presence of GSNO (10 μM) for 15 days. (C) HT1080 cells ($\sim 2 \times 10^4$) were treated with both 6-TG (1 μM) and GSNO (10 μM) for 15 days. The co-IP of Ras from these cells and preparation of the nucleotide(s) released from the co-IPed Ras sample are described in Materials and Methods. The sample containing Ras-released nucleotide(s) from the co-IPed Ras was analyzed with ESI-MS to determine if the Ras isolated from cells releases chemically modified nucleotide(s). (D) An end product of kinetic assays (i.e., TGDP-bound G12V-SNO Ras treated with $^{\bullet}NO_2$) was analyzed by ESI-MS essentially as described in the previous study (*22*).

Kinetic Properties of Ras GTPases with TGNP in the Presence and Absence of RNS. To better understand Ras TGNP binding interactions, the apparent dissociation constant ($^{app}K_D$) of the non-S-nitrosated wt, G12V, and Q61K Ras for TGDP at 25 °C was determined to be 17.9, 16.0, and 23 μM, respectively (Figure 7A). These Ras mutants G12V and Q61K, in addition to wt Ras, were chosen for the binding study because they have been identified as a cellular target of TGNP (derived from treated 6-TG) in T24 and HT1080 cells, respectively (Figure 5). The $^{app}K_D$ values of Ras G12V and Q61K for TGDP do not significantly differ from that of wt Ras for TGDP. The $^{app}K_D$ value of wt Ras for TGDP is slightly larger than that of wt Ras for GDP (*57*). As shown in Figure 7B, TGDP competes with GDP for the nucleotide-binding site of wt, G12V, and Q61K Ras. The study of competitive binding also estimates a true dissociation constant ($^{true}K_D$) of wt Ras for TGDP as ~32 pM (Figure 7B), which is ~3.5-fold larger than that for GDP (*75*). The $^{true}K_D$ values of G12V and Q61K Ras for TGDP are likely to be similar to that of wt Ras because $^{app}K_D$ and apparent-competitive K_D values ($^{app\text{-}comp}K_{D\,TGDP}$) are similar to that of wt Ras. These results and analyses suggest that, similar to GNP, TGNP has a high affinity for binding to wt, G12V, and Q61K Ras proteins. These binding results also explain the presence of TGNP, as a ligand of Ras, in thiopurine-treated T24 and HT1080 cells (Figure 5A).

The redox property of the Ras-TGDP complex was examined *in vitro* as a way to assess the possible link between the Ras-bound TGNP and cell apoptosis under the NO-mediated oxidative stress conditions. Because Ras in these cells treated with GSNO or DETA/NO was S-nitrosated (Figure 2), Ras G12V-SNO and Q61K-SNO were used for the assay. Figure 8 shows that although the Ras G12V-SNO GTPase was redox inactive, $^{\bullet}NO_2$ enhances the dissociation of the bound TGDP from the Ras-SNO G12V protein. The end product analysis using ESI-MS showed that, upon treatment with $^{\bullet}NO_2$ (Figure 5D), the bound TGDP was dissociated from Ras-SNO G12V as a form of NIm-DP (463.3 Da). $^{\bullet}NO_2$ also enhances the dissociation of the bound TGDP from

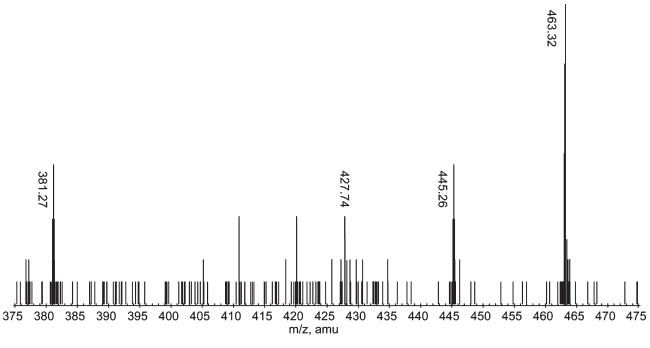

FIGURE 6: Tandem mass spectrometry analysis of the RNS-mediated Ras-bound TGNP dissociation product. An aliquot of the co-IPed Ras sample (Figure 5) was analyzed by employing MS/MS. Mass peaks, 381.3, 427.7, and 445.3 Da, corresponding to NIm-DP fragments are shown (*22*).

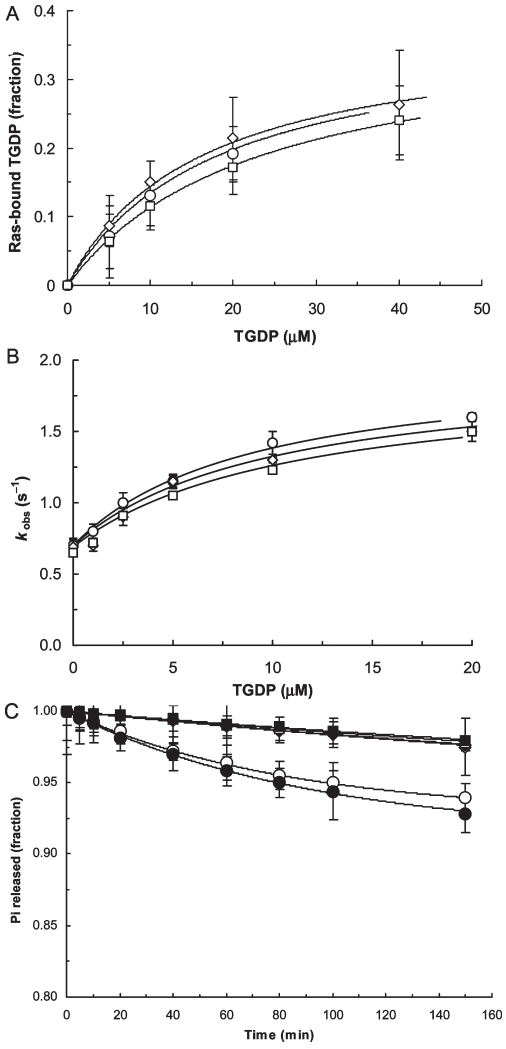

FIGURE 7: Kinetic properties of Ras TGDP-binding interactions. The Materials and Methods section contains descriptions of methods to determine the dissociation constants of Ras GTPases for TGDP, the competitive dissociation constants of Ras for TGDP with mantGDP, and the GTPase activity of Ras for TGDP. (A) $^{app}K_D$ values of non-S-nitrosated wt (○), G12V (◇), and Q61K (□) Ras GTPases for TGDP were then estimated to be 17.9, 16.0, and 23.0 μM, respectively, by using Prism software to fit the plot to one site-binding association (hyperbola). (B) The apparent competitive K_D values ($^{app\text{-}comp}K_{D\,TGDP}$) of non-S-nitrosated wt (○), G12V (◇), and Q61K (□) Ras GTPases for TGDP were determined to be 9.1, 10.8, and 10.4 μM, respectively. The true K_D value of the non-S-nitrosated wt Ras for GDP ($^{true}K_{D\,GDP}$) was known to be ~9 pM (*75*). The true K_D value of the non-S-nitrosated wt Ras for TGDP ($^{true}K_{D\,TGDP}$) was then calculated to be ~32 pM by using a compensation equation, $^{true}K_{D\,TGDP} = {}^{app\text{-}comp}K_{D\,TGDP}/(1 + [mantGDP]/{}^{true}K_{D\,GDP})$ (*95*), in conjunction with the values given {($^{app\text{-}comp}K_{D\,TGDP} = 9.1$ μM, [mantGDP] = 2.5 μM, and $^{true}K_{D\,GDP} = \sim 9$ pM. $\therefore$ $^{true}K_{D\,TGDP} = 9.1$ μM/(1 + 2.5 μM mantGDP/~9 pM) = ~32 pM}. Because the $^{true}K_{D\,GDP}$ values for G12V and Q61K Ras are not reported, the $^{true}K_{D\,TGDP}$ values for G12V and Q61K were not calculated. (C) The rates of P_i released from the TGTP-bound non-S-nitrosated wt (●), G12V (◆), and Q61K (■) Ras GTPases were estimated to be 1.08×10^{-2}, 0.21×10^{-2}, and 0.20×10^{-2} s^{-1}, respectively, by using Prism software to fit the plot to one-phase exponential dissociation. The rates of P_i released from GTP-bound non-S-nitrosated wt (○), G12V (◇), and Q61K (□) Ras GTPases also were estimated to be 1.20×10^{-2}, 0.21×10^{-2}, and 0.19×10^{-2} s^{-1}, respectively, by using Prism software to fit the plot to a one-phase exponential dissociation. The regression (r^2) values associated with these fits were > 0.7585. The data presented in these figures by vertical standard error bars are the mean values of triplicate measurements.

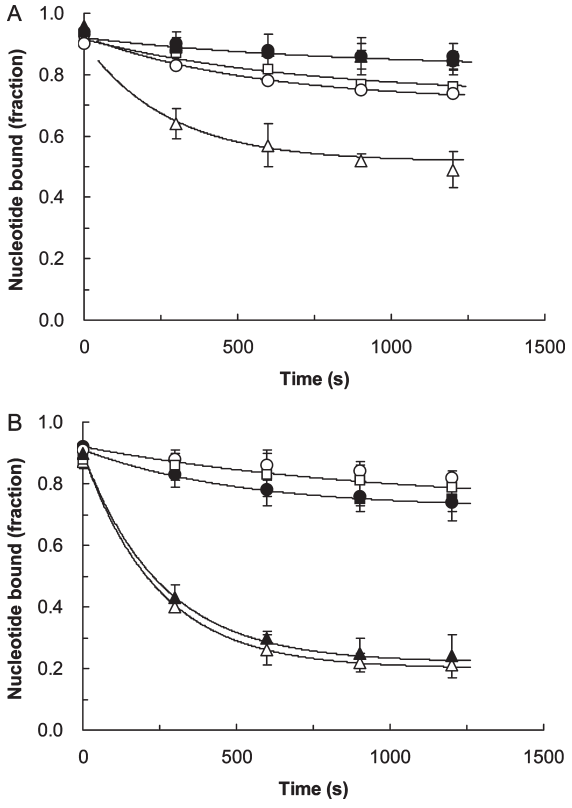

FIGURE 8: Kinetic properties of GDP- or TGDP-bound Ras GTPases in the presence of various RNS. The method to determine the effect of RNS on TGDP-bound Ras was described in Materials and Methods. (A) The estimated GDP dissociation rates from Ras G12V in the presence of •NO (○), $^{\bullet}NO_2$ (△), and N_2O_3 (□) were determined to be 0.18×10^{-3}, 3.72×10^{-3}, and 0.14×10^{-3} s^{-1}, respectively. Rates for GDP dissociation from Ras-SNO G12V by •NO (●), $^{\bullet}NO_2$ (▲), and N_2O_3 (■) were estimated to be 0.09×10^{-3}, 0.13×10^{-3}, and 0.10×10^{-3} s^{-1}, respectively. (B) The rates of dissociation of TGDP from Ras-SNO G12V mediated by •NO (○), $^{\bullet}NO_2$ (△), and N_2O_3 (□) were determined to be 0.10×10^{-3}, 3.94×10^{-3}, and 0.12×10^{-3} s^{-1}, respectively. The Ras C118S TGDP dissociation rates in the presence of •NO (●), $^{\bullet}NO_2$ (▲), and N_2O_3 (■) were determined to be 0.13×10^{-3}, 4.18×10^{-3}, and 0.14×10^{-3} s^{-1}, respectively. Each data point and bar in the figure indicate respectively the mean values of triplicate measurements and the corresponding standard errors. The r^2 values of all fits were > 0.9605.

the redox-inactive Ras Q61K-SNO GTPase (not shown). The dissociation rates of wt un-S-nitrosated Ras-bound TGDP as a consequence of treatment with other RNS such as NO and N_2O_3 were minimal (not shown). The effects of RNS, including NO, $^{\bullet}NO_2$, and N_2O_3, on TGDP complexed with another Ras redox-inactive mutant C118S were also examined. $^{\bullet}NO_2$ effectively enhances dissociation of TGDP from the redox mutant Ras GTPase, but NO and N_2O_3 were ineffective (Figure 8). Like the end product of the $^{\bullet}NO_2$-treated TGDP-bound Ras-SNO G12V, end products of the $^{\bullet}NO_2$-treated TGDP-bound wt Ras-SNO, C118S, or Q61K-SNO Ras were identified as NIm-DP (not shown). The rate difference between the oncogenic Ras-SNO TGDP dissociation (this study) and the redox-active Ras GTPase GDP dissociation was insignificant (*22*). No further enhancement of the dissociation rate of TGDP occurred, even if Ras was redox active (not shown).

These kinetic results support findings from the cell study that the redox-inactive Ras (i.e., all Ras-SNO forms and Ras C118S) resumes its redox responses to $^{\bullet}NO_2$ by binding with TGNP and that the end product of the process is NIm-DP.

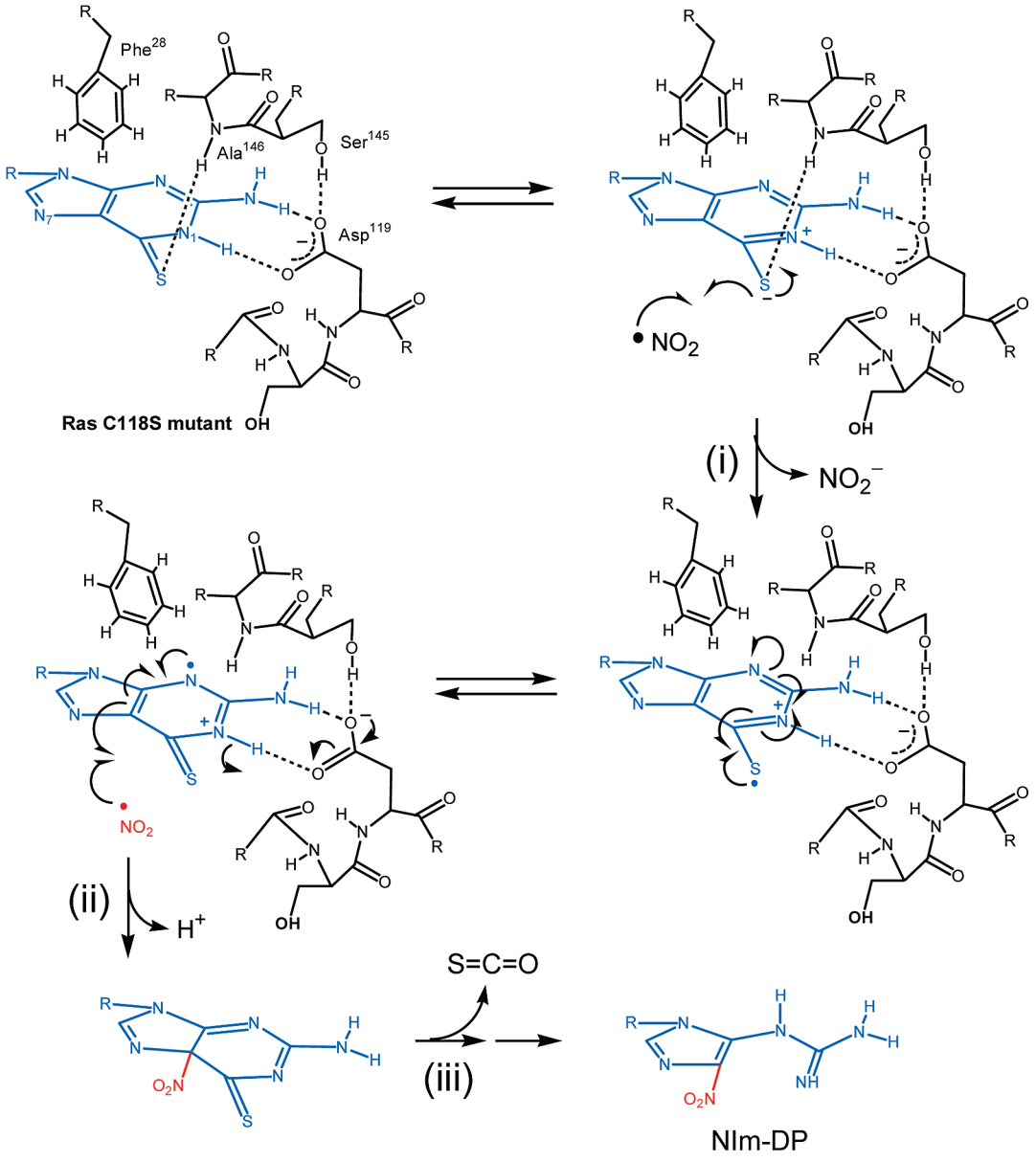

FIGURE 9: Proposed mechanism of RNS-mediated Ras TGNP dissociation. TGNP and redox-inactive Ras C118S are represented in blue and black, respectively, and the NO_2 moiety of the nucleotide-nitration adduct is shown in red. The ribose phosphate moiety of TGNP is depicted by R. The black dotted lines represent putative hydrogen bond interactions between Ras residues and TGNP.

Potential Mechanism for the Conversion of Ras-Bound TGNP into NIm-DP. The molecular mechanism for the release of TGNP from the redox-inactive Ras associated with release of NIm-DP in the presence RNS is of interest because it determines, in part, a potential path for thiopurine drugs associated with Ras.

As noted elsewhere, the only difference between GNP and TGNP is the atom on C_6 of the nucleotide base; TGNP possesses a sulfur atom at this site, but GNP has an oxygen atom (*11*). $^{\bullet}NO_2$, but neither NO nor N_2O_3, reacts directly with the sulfur atom on glutathione anion and cysteine to produce a thiyl radical (*19*−*21*). Hence, the sulfur atom of TGNP may react with $^{\bullet}NO_2$ to produce a TGNP-thiyl radical. Moreover, the Ras GNP crystal structure shows that the C_6 oxygen of the bound GNP is exposed to solvent (*76*−*78*), suggesting that the C_6 sulfur atom of the Ras-bound TGNP is likely to be accessible with a solvent. Therefore, the sulfur atom of TGNP, as a Ras-bound form, can be a direct target of $^{\bullet}NO_2$ so as to produce a TGNP-thiyl radical. Except for the C_6 sulfur atom, the base structure of TGNP is identical to that of GNP (*11*).

It has been suggested that hydrogen-bonding interactions between the bound GNP base and Ras switches I and II result in perturbation of the electronic state of the bound GNP base (*22*). Therefore, like GNP, the electronic state of the bound TGNP base is likely to be perturbed when it binds to Ras. This could lead to lowering the redox potential of the TGNP base, making the sulfur atom of TGNP more reactive to $^{\bullet}NO_2$ to produce a Ras-bound TGNP-thiyl radical. If so, the TGNP-thiyl radical then proceeds to disturb the Ras-binding interactions with TGNP (Figure 9). The process of this binding interaction perturbation is enhanced by the reaction of the TGNP-thiyl radical with another $^{\bullet}NO_2$, resulting at last in release of a chemically modified TGNP, a TGNP-NO_2 adduct. Notably, the TGNP-thiyl radical (Figure 9) is chemically equivalent to the oxygen radical in the radical-based Ras nucleotide dissociation mechanism (*22*). Moreover, the postulated molecular mechanism for dissociation of the bound TGNP from Ras-SNO G12V as TGNP-NO_2 is essentially the same as that of the second state of the radical-based mechanism of GNP dissociation from the

redox-active Ras GTPase (*22*). However, it skips one step, which is the Ras protein-radical state proposed for the radical-based Ras nucleotide dissociation mechanism. The unstable TGNP-NO_2 is degraded into NIm-DP through release of a carbon oxide sulfide (O═C═S). The mechanism by which NIm-DP is formed from the TGDP-NO_2 adduct by releasing O═C═S is likely to be similar to the decarboxylation of GDP-NO_2 to produce NIm-DP (*22*).

DISCUSSION

Prodrug thiopurines can be converted into biologically active TdGNP and TGNP (*1*−*3*, *8*−*10*). Although the therapeutic action of TdGNP is well-known (*1*−*7*), little research has been devoted to the cellular action(s) of TGNP in either the presence or absence of RNS.

Cellular Path of TGNP in the Presence of RNS. This study uses tumor cell lines to show that TGNP can target Ras GTPases, a finding that is consistent with previous studies (*8*, *9*). Although the action of TdGNP in targeting DNA is immediate (*10*, *12*−*14*), the cellular action of TGNP in targeting Ras is gradual and requires an assist from redox agent(s) such as RNS. Although tumor cells develop resistance to thiopurines over a course of treatment, the Ras ligand GNP also is replaced with TGNP. Long-term treatment of these tumor cells with RNS produced a form of redox-inactive Ras-SNO. The TGNP bound to Ras-SNO was converted in the presence of RNS into NIm-DP, which couples with inactivation of Ras and its downstream effector protein Raf-1.

This study also shows that RNS induces apoptosis of the thiopurine-resistant tumor cells. Several studies have shown that downregulation of HRas in T24 cells results in a decrease in the proliferative capacity of the T24 cells (*61*−*64*). It also has been demonstrated that NRas Q61K plays a key role in the aggressive tumorigenic growth of HT1080 cells (*79*, *80*). Therefore, given that RNS downregulates the constitutively active oncogenic Ras protein in the thiopurine-resistant tumor cells, we propose that the oncogenic Ras targeting action of RNS results in apoptosis and deters the growth of thiopurine-resistant T24 and HT1080 cells.

Implication of the Action of RNS on the Thiopurine-Resistant Tumor Cells. Cytotoxic effects associated with chronic exposure to thiopurine drugs are all but inevitable (*7*, *10*, *15*−*18*). The thiopurine cytotoxicities associated with the DNA-targeting TdGNP are well-known (*7*, *15*−*18*). This is not true of the thiopurine cytotoxicities associated with the cellular protein-targeting TGNP. This study is the first to demonstrate that an accumulation of TGNP over the course of long-term treatment with thiopurines can interfere with cellular protein Ras GTPases in the presence of RNS. Given that Ras plays a key role in cell signaling events, deregulation and/or misregulation of Ras is detrimental and thus cytotoxic to cells.

Potential Effect of Thiopurine-Mediated Depletion of Glutathione on the Action of RNS on TGNP-Bound Ras Proteins. GSH depletion also has been shown to render thiopurines cytotoxic (*81*−*83*). GSH serves as a redox buffer that can quench ROS and RNS (*84*−*86*), and thus a decrease in the cellular concentration of GSH could enhance the effect of RNS.

Depletion of GSH may push the level of ROS (e.g., $O_2^{\bullet-}$) in cells treated with thiopurines higher than in untreated cells. Given that ROS can oxidize thiol/thiolate-containing biomolecules such as cysteines (*87*), oxidation of the Ras Cys^{118} side chain can occur after cells are treated with thiopurines. Although barely detectable, the peak intensities associated with the oxidized Ras Cys^{118} side chains (a form of sulfenic acid, but some also were in the form of sulfinic and sulfonic acids) were unchanged after cells were treated with 6-thioguanine and GSNO (or DETA/NO). Also, we have previously shown that $O_2^{\bullet-}$ (or $OH^{\bullet}$) can enhance Ras guanine nucleotide dissociation and that oxidized guanine nucleotide derivatives are the resultant end products (*23*, *25*). Therefore, detection of mass signatures of oxidized nucleotide derivatives (i.e., imidazolone) (*23*, *25*, *88*) can be expected in mass spectroscopic analyses of Ras samples from cells treated with 6-thiopurines. We were unable to identify any mass peaks assigned to oxidized guanine nucleotide derivatives.

Although our results failed to support a potential role for ROS in cells treated with thiopurines, our results may imply an indirect role of ROS in conjunction with RNS in cells treated with thiopurines. For example, because cells were treated with both thiopurine and NO, both unquenched $O_2^{\bullet-}$ and NO will be present in cells. $O_2^{\bullet-}$ can be quenched by its reaction with NO to produce $ONOO^-$. Although $ONOO^-$ is a direct precursor of $^{\bullet}NO_2$ and $OH^{\bullet}$ (*28*), the $ONOO^-$ that is formed then further reacts with CO_2 to produce $^{\bullet}NO_2$ and $CO_3^{\bullet-}$ (*32*). Because our cell culture system uses atmospheric CO_2 (5%) to maintain a cell culture pH, $CO_3^{\bullet-}$ but not $OH^{\bullet}$ is likely to be the dominant presence in our cell system. These analyses serve to explain why the effect of $O_2^{\bullet-}$ *per se* on cells in conjunction with thiopurines was not readily dominant. Because the redox potential of $CO_3^{\bullet-}$ exceeds that of $^{\bullet}NO_2$ (*89*), $CO_3^{\bullet-}$ can oxidize the bound TGNP. A study shows that a treatment of a guanine base with $CO_3^{\bullet-}$ and then with $^{\bullet}NO_2$ produces a NO_2-guanine adduct (*90*). These results and analyses suggest that, under our experimental conditions (in the presence of CO_2), the 6-thioguanine-induced depletion of GSH creates a favorable cellular environment for $^{\bullet}NO_2$ action that targets the Ras-bound TGNP.

Because CO_2 is minimally present under *in vivo* conditions, our cell study result and analysis may not be directly applicable to living organisms (i.e., human patients). In the absence of CO_2, $OH^{\bullet}$, in addition to $^{\bullet}NO_2$, instead of $CO_3^{\bullet-}$, is produced from the decomposition of $ONOO^-$ (*28*). Because the redox potential of $OH^{\bullet}$ is relatively high, $OH^{\bullet}$ *per se* is considered a serious cytotoxic redox agent (*26*). Hence, under *in vivo* conditions (lack of CO_2), the depletion of GSH as the result of treatment with 6-thioguanine produces not only a cytotoxic $OH^{\bullet}$ but also more $^{\bullet}NO_2$ that can target the TGNP bound to Ras. Production of more $^{\bullet}NO_2$ could cause dysregulation of Ras and its signaling events with results that are cytotoxic to cells.

Insight into the Cellular Mechanism and the Redox-Mediated Ras Inactivation in Thiopurine-Treated Cells. The proposed molecular mechanism (Figure 9) for formation of NIm-DP is based upon end product analyses. However, the proposed thiopurine radical intermediate has not been either trapped or identified. Consequently, how the putative Ras-bound thiopurine radical intermediate perturbs the Ras guanine nucleotide-binding interaction remains speculative.

Although further research is necessary for validation, the molecular mechanism (Figure 9) in conjunction with *in vitro* kinetic studies further serves to explain, in part, the cell study results associated with the effect of thiopurines in the presence of RNS. However, the role, if any, of the metabolic path of NIm-DP is unclear. Further studies are required to delineate the cellular role and path of NIm-DP.

The K_D of Ras with NIm-DP is too large to determine accurately. This is most likely because NIm-DP lacks the complete

architecture of the purine base that would permit it to form hydrogen-bonding interactions with the Ras NKCD motif. The analysis suggests that NIm-DP cannot compete with other nucleotides, i.e., GNP or TGNP, in binding with Ras. However, the results of this analysis conflict with the finding that, in the presence of RNS, Ras was able to probe NIm-DP, as a ligand, from the pool of various cellular nucleotides. A possible explanation for this contradiction is that the probed Ras-bound ligand first existed as TGNP-NO_2. Also, because TGDP-NO_2 conserves its purine base, TGDP-NO_2 predictably can bind to Ras as tightly as to TGNP. Hence, a fraction of the Ras-released TGDP-NO_2 may rebind to Ras to produce the Ras-TGNP-NO_2 complex. However, once TGNP-NO_2 was probed with Ras and released from it for mass analysis (by using ESI-MS) under our experimental conditions, it was likely to be converted into NIm-DP because the free form of TGNP-NO_2 is unstable.

Because the γ-phosphate of TGTP is unstable at room temperature, TGDP was used for the *in vitro* kinetic experiments, and thus, the model mechanism (Figure 9) was proposed for the interaction of Ras TGDP in the presence of RNS. The cellular ratio of GTP/GDP is ~10 (*91*). Because the metabolic path that guanine takes to produce nucleotides is shared with 6-TG (*3*, *8*−*10*, *92*), the ratio of TGTP/TGDP is likely to be similar to that of GTP/GDP (*91*). Hence, TGTP is most likely the primary nucleotide species in the cell, and thus TGTP-bound Ras is likely to be populated in a cell treated with 6-TG. If so, TGTP, but not TGDP, will be prevalent to react with $^{\bullet}NO_2$ to produce the TGTP-NO_2 adduct, which would be converted into 5-guanidino-4-nitroimidazole triphosphate (NIm-TP).

This analysis contradicts the results in Figure 5A in which Ras is shown as forming a complex with TGDP but not with TGTP. Moreover, Figure 5B,C mainly identifies NIm-DP but not NIm-TP. The best explanation for this enigmatic result is that, because the γ-phosphate of GTP and TGTP-NO_2 adduct (and/or its decarboxylated form NIm-TP) is thermodynamically unstable in its free form, the Ras-released TGTP and TGTP-NO_2/NIm-TP are converted into TGDP and TGDP-NO_2/NIm-DP during our experimental procedures (immunoprecipitation and subsequent ESI-MS analysis). These procedures were undertaken to detect Ras-bound nucleotides in cells in the presence or absence of RNS.

A redox agent (i.e., NO or $^{\bullet}NO_2$), like GEFs, facilitates the equilibrium between GNP bound to Ras and cellular free GNP by enhancing dissociation of the bound nucleotide, and the cellularly abundant GTP binds to Ras to produce active GTP-bound Ras (*22*, *23*, *25*). The redox agent- or GEF-mediated dissociation process is not selective for GDP over GTP; thus it is expected that the action of a redox agent is not selective for TGDP over TGTP. In accounting for the proposed mechanism (Figure 9), the equilibrium between the cellular TGNP and the TGNP-bound G12V-SNO or G61K-SNO Ras can also be enhanced by $^{\bullet}NO_2$. However, less clear is how $^{\bullet}NO_2$ inactivates the TGNP-bound G12V-SNO or G61K-SNO Ras. Intriguingly, previous studies show that, although the mechanism is unclear, in some cases a redox agent acts on Ras in a reverse manner, as when a redox agent inactivates Ras in N293 cells (HEK-293 transfected with neuronal nitric oxide synthase) (*74*, *93*) or in human pulmonary arterial smooth muscle cells (*94*).

Enhancement of the equilibrium between the cellularly free TGNP and the oncogenic Ras-bound TGNP cannot serve to inactivate Ras unless the cellular ratio of TGTP/TGDP is $\ll 1$. Another possibility is that a redox agent (i.e., $^{\bullet}NO_2$) and Ras downstream effector proteins compete for the TGTP-bound Ras. Therefore, somehow the presence of RNS serves to reduce a portion of the mechanically stable state of oncogenic Ras-SNO that is bound with TGTP and capable of interacting with its downstream effector proteins. Further studies are required to clarify the redox agent-mediated inactivation of the TGNP-bound Ras-SNO.

CONCLUDING REMARKS

This study attempts to define the effect of TGNP derived from thiopurine drugs on Ras by using Ras-activated cancer cell lines that are under RNS-mediated oxidative stress. However, given that TGNP can be a ligand for other small GTPases, including Rho proteins and heterotrimeric GTPases, the results provided herein may be applicable to other GTPases.

Although previous studies show that TGNP derived from thiopurines targets Rho GTPases (*8*, *9*), its action on Rho GTPases associated with RNS and/or ROS has not been investigated. Further studies of the action of TGNP on other GNP-binding proteins such as the Rho family and multimeric GTPases are required for a better understanding of the thiopurine-mediated GTPase-targeting cytotoxic and/or therapeutic effect(s).

ACKNOWLEDGMENT

We thank Dr. Alfred Wittinghofer at the Max-Planck-Institut in Germany for providing HRas 1−166 and HRas C118S. We also thank Dr. Osamu Yamamoto at the Systems and Structural Biology Center, Riken, Japan, for providing the Ras binding domain of the Raf-1 construct used in this study.

REFERENCES

1. Elion, G. B. (1989) The purine path to chemotherapy. *Science 244*, 41–47.
2. Langmuir, P. B., Aplenc, R., and Lange, B. J. (2001) Acute myeloid leukaemia in children. *Best Pract. Res. Clin. Haematol. 14*, 77–93.
3. Gearry, R. B., and Barclay, M. L. (2005) Azathioprine and 6-mercaptopurine pharmacogenetics and metabolite monitoring in inflammatory bowel disease. *J. Gastroenterol. Hepatol. 20*, 1149–1157.
4. Penn, I. (1993) Incidence and treatment of neoplasia after transplantation. *J. Heart Lung Transplant 12*, S328–336.
5. Larson, R. S., Manning, S., Macon, W. R., and Vnencak-Jones, C. (1997) Microsatellite instability in natural killer cell-like T-cell lymphomas in immunocompromised and immunocompetent individuals. *Blood 89*, 1114–1115.
6. Offman, J., Opelz, G., Doehler, B., Cummins, D., Halil, O., Banner, N. R., Burke, M. M., Sullivan, D., Macpherson, P., and Karran, P. (2004) Defective DNA mismatch repair in acute myeloid leukemia/myelodysplastic syndrome after organ transplantation. *Blood 104*, 822–828.
7. Karran, P. (2006) Thiopurines, DNA damage, DNA repair and therapy-related cancer. *Br. Med. Bull. 79*−*80*, 153–170.
8. Tiede, I., Fritz, G., Strand, S., Poppe, D., Dvorsky, R., Strand, D., Lehr, H. A., Wirtz, S., Becker, C., Atreya, R., Mudter, J., Hildner, K., Bartsch, B., Holtmann, M., Blumberg, R., Walczak, H., Iven, H., Galle, P. R., Ahmadian, M. R., and Neurath, M. F. (2003) CD28-dependent Rac1 activation is the molecular target of azathioprine in primary human CD4+ T lymphocytes. *J. Clin. Invest. 111*, 1133–1145.
9. de Boer, N. K., van Bodegraven, A. A., Jharap, B., de Graaf, P., and Mulder, C. J. (2007) Drug insight: pharmacology and toxicity of thiopurine therapy in patients with IBD. *Nat. Clin. Pract. Gastroenterol. Hepatol. 4*, 686–694.
10. Petit, E., Langouet, S., Akhdar, H., Nicolas-Nicolaz, C., Guillouzo, A., and Morel, F. (2008) Differential toxic effects of azathioprine, 6-mercaptopurine and 6-thioguanine on human hepatocytes. *Toxicol. In Vitro 22*, 632–642.
11. Weng, G., Chen, C. X., Balogh-Nair, V., Callender, R., and Manor, D. (1994) Hydrogen bond interactions of G proteins with the guanine ring moiety of guanine nucleotides. *Protein Sci. 3*, 22–29.
12. Lage, H., and Dietel, M. (1999) Involvement of the DNA mismatch repair system in antineoplastic drug resistance. *J. Cancer Res. Clin. Oncol. 125*, 156–165.

13. Yan, T., Berry, S. E., Desai, A. B., and Kinsella, T. J. (2003) DNA mismatch repair (MMR) mediates 6-thioguanine genotoxicity by introducing single-strand breaks to signal a G2-M arrest in MMR-proficient RKO cells. *Clin. Cancer Res. 9*, 2327–2334.
14. Karran, P., and Attard, N. (2008) Thiopurines in current medical practice: molecular mechanisms and contributions to therapy-related cancer. *Nat. Rev. Cancer 8*, 24–36.
15. Hsieh, P., and Yamane, K. (2008) DNA mismatch repair: molecular mechanism, cancer, and ageing. *Mech. Ageing Dev. 129*, 391–407.
16. Casorelli, I., Russo, M. T., and Bignami, M. (2008) Role of mismatch repair and MGMT in response to anticancer therapies. *Anticancer Agents Med. Chem. 8*, 368–380.
17. O'Donovan, P., Perrett, C. M., Zhang, X., Montaner, B., Xu, Y. Z., Harwood, C. A., McGregor, J. M., Walker, S. L., Hanaoka, F., and Karran, P. (2005) Azathioprine and UVA light generate mutagenic oxidative DNA damage. *Science 309*, 1871–1874.
18. Daehn, I., and Karran, P. (2009) Immune effector cells produce lethal DNA damage in cells treated with a thiopurine. *Cancer Res. 69*, 2393–2399.
19. Ford, E., Hughes, M., and Wardman, P. (2002) Kinetics of the reactions of nitrogen dioxide with glutathione, cysteine, and uric acid at physiological pH. *Free Radical Biol. Med. 32*, 1314–1323.
20. Jourd'heuil, D., Jourd'heuil, F., and Feelisch, M. (2003) Oxidation and nitrosation of thiols at low micromolar exposure to nitric oxide. Evidence for a free radical mechanism. *J. Biol. Chem. 278*, 15720–15726.
21. Schrammel, A., Gorren, A., Schmidt, K., Pfeiffer, S., and Mayer, B. (2003) S-nitrosation of glutathione by nitric oxide, peroxynitrite, and NO/O_2. *Free Radical Biol. Med. 34*, 1078–1088.
22. Heo, J., Prutzman, K. C., Mocanu, V., and Campbell, S. L. (2005) Mechanism of free radical nitric oxide-mediated Ras guanine nucleotide dissociation. *J. Mol. Biol. 346*, 1423–1440.
23. Heo, J., and Campbell, S. L. (2005) Superoxide anion radical modulates the activity of Ras and Ras-related GTPases by a radical-based mechanism similar to that of nitric oxide. *J. Biol. Chem. 280*, 12438–12445.
24. Heo, J., and Campbell, S. L. (2005) Mechanism of redox-mediated guanine nucleotide exchange on redox-active Rho GTPases. *J. Biol. Chem. 280*, 31003–31010.
25. Heo, J., and Campbell, S. L. (2006) Ras regulation by reactive oxygen and nitrogen species. *Biochemistry 45*, 2200–2210.
26. Augusto, O., Bonini, M. G., Amanso, A. M., Linares, E., Santos, C. C., and De Menezes, S. L. (2002) Nitrogen dioxide and carbonate radical anion: two emerging radicals in biology. *Free Radical Biol. Med. 32*, 841–859.
27. Heo, J., and Campbell, S. L. (2004) Mechanism of $p21^{Ras}$ S-nitrosylation and kinetics of nitric oxide-mediated guanine nucleotide exchange. *Biochemistry 43*, 2314–2322.
28. Goldstein, S., Lind, J., and Merenyi, G. (2005) Chemistry of peroxynitrites as compared to peroxynitrates. *Chem. Rev. 105*, 2457–2470.
29. Koppenol, W. H. (1998) The basic chemistry of nitrogen monoxide and peroxynitrite. *Free Radical Biol. Med. 25*, 385–391.
30. Ronson, R. S., Nakamura, M., and Vinten-Johansen, J. (1999) The cardiovascular effects and implications of peroxynitrite. *Cardiovasc. Res. 44*, 47–59.
31. Windholz, M., Budavari, S., Blumetti, R. F., and Otterbein, E. S., Eds. (1983) The Merck Index, 10th ed., Merck & Co., Rahway, NJ.
32. Bonini, M. G., Radi, R., Ferrer-Sueta, G., Ferreira, A. M., and Augusto, O. (1999) Direct EPR detection of the carbonate radical anion produced from peroxynitrite and carbon dioxide. *J. Biol. Chem. 274*, 10802–10806.
33. Poppe, D., Tiede, I., Fritz, G., Becker, C., Bartsch, B., Wirtz, S., Strand, D., Tanaka, S., Galle, P. R., Bustelo, X. R., and Neurath, M. F. (2006) Azathioprine suppresses ezrin-radixin-moesin-dependent T cell-APC conjugation through inhibition of Vav guanosine exchange activity on Rac proteins. *J. Immunol. 176*, 640–651.
34. Geyer, M., and Wittinghofer, A. (1997) GEFs, GAPs, GDIs and effectors: taking a closer (3D) look at the regulation of Ras-related GTP-binding proteins. *Curr. Opin. Struct. Biol. 7*, 786–792.
35. Sprang, S. (2001) GEFs: master regulators of G-protein activation. *Trends Biochem. Sci. 26*, 266–267.
36. Adachi, T., Pimentel, D. R., Heibeck, T., Hou, X., Lee, Y. J., Jiang, B., Ido, Y., and Cohen, R. A. (2004) S-glutathiolation of Ras mediates redox-sensitive signaling by angiotensin II in vascular smooth muscle cells. *J. Biol. Chem. 279*, 29857–29862.
37. Baker, T., Booden, M., and Buss, J. (2000) S-Nitrosocysteine increases palmitate turnover on Ha-Ras in NIH 3T3 cells. *J. Biol. Chem. 275*, 22037–22047.
38. Lander, H. M., Hajjar, D. P., Hempstead, B. L., Mirza, U. A., Chait, B. T., Campbell, S. L., and Quilliam, L. A. (1997) A molecular redox switch on $p21^{ras}$. Structural basis for the nitric oxide-$p21^{ras}$ interaction. *J. Biol. Chem. 272*, 4323–4326.
39. Lander, H. M., Ogiste, J. S., Pearce, S. F., Levi, R., and Novogrodsky, A. (1995) Nitric oxide-stimulated guanine nucleotide exchange on $p21^{ras}$. *J. Biol. Chem. 270*, 7017–7020.
40. Mitsushita, J., Lambeth, J. D., and Kamata, T. (2004) The superoxide-generating oxidase Nox1 is functionally required for Ras oncogene transformation. *Cancer Res. 64*, 3580–3585.
41. Chuang, J. I., Chang, T. Y., and Liu, H. S. (2003) Glutathione depletion-induced apoptosis of Ha-ras-transformed NIH3T3 cells can be prevented by melatonin. *Oncogene 22*, 1349–1357.
42. Nimnual, A. S., Taylor, L. J., and Bar-Sagi, D. (2003) Redox-dependent downregulation of Rho by Rac. *Nat. Cell Biol. 5*, 236–241.
43. Dawson, T. M., Sasaki, M., Gonzalez-Zulueta, M., and Dawson, V. L. (1998) Regulation of neuronal nitric oxide synthase and identification of novel nitric oxide signaling pathways. *Prog. Brain Res. 118*, 3–11.
44. Gonzalez-Zulueta, M., Feldman, A. B., Klesse, L. J., Kalb, R. G., Dillman, J. F., Parada, L. F., Dawson, T. M., and Dawson, V. L. (2000) Requirement for nitric oxide activation of p21(ras)/extracellular regulated kinase in neuronal ischemic preconditioning. *Proc. Natl. Acad. Sci. U.S.A. 97*, 436–441.
45. Bosworth, C. A., Toledo, J. C., Jr., Zmijewski, J. W., Li, Q., and Lancaster, J. R., Jr. (2009) Dinitrosyliron complexes and the mechanism(s) of cellular protein nitrosothiol formation from nitric oxide. *Proc. Natl. Acad. Sci. U.S.A. 106*, 4671–4676.
46. Maragos, C. M., Morley, D., Wink, D. A., Dunams, T. M., Saavedra, J. E., Hoffman, A., Bove, A. A., Isaac, L., Hrabie, J. A., and Keefer, L. K. (1991) Complexes of .NO with nucleophiles as agents for the controlled biological release of nitric oxide. Vasorelaxant effects. *J. Med. Chem. 34*, 3242–3247.
47. Mooradian, D. L., Hutsell, T. C., and Keefer, L. K. (1995) Nitric oxide (NO) donor molecules: effect of NO release rate on vascular smooth muscle cell proliferation in vitro. *J. Cardiovasc. Pharmacol. 25*, 674–678.
48. Floryszak-Wieczorek, J., Milczarek, G., Arasimowicz, M., and Ciszewski, A. (2006) Do nitric oxide donors mimic endogenous NO-related response in plants? *Planta 224*, 1363–1372.
49. Vistica, D. T., Skehan, P., Scudiero, D., Monks, A., Pittman, A., and Boyd, M. R. (1991) Tetrazolium-based assays for cellular viability: a critical examination of selected parameters affecting formazan production. *Cancer Res. 51*, 2515–2520.
50. Sato, M., Kawamata, H., Harada, K., Nakashiro, K., Ikeda, Y., Gohda, H., Yoshida, H., Nishida, T., Ono, K., Kinoshita, M., and Adachi, M. (1997) Induction of cyclin-dependent kinase inhibitor, p21WAF1, by treatment with 3,4-dihydro-6-[4-(3,4)-dimethoxybenzoyl)-1-piperazinyl]-2(1*H*)-quinoline (vesnarinone) in a human salivary cancer cell line with mutant p53 gene. *Cancer Lett. 112*, 181–189.
51. Yamashita, A., Hakura, A., and Inoue, H. (1999) Suppression of anchorage-independent growth of human cancer cell lines by the drs gene. *Oncogene 18*, 4777–4787.
52. Ghatak, S., Misra, S., and Toole, B. P. (2002) Hyaluronan oligosaccharides inhibit anchorage-independent growth of tumor cells by suppressing the phosphoinositide 3-kinase/Akt cell survival pathway. *J. Biol. Chem. 277*, 38013–38020.
53. de Rooij, J., and Bos, J. L. (1997) Minimal Ras-binding domain of Raf1 can be used as an activation-specific probe for Ras. *Oncogene 14*, 623–625.
54. Reinstein, J., Schlichting, I., Frech, M., Goody, R. S., and Wittinghofer, A. (1991) p21 with a phenylalanine 28−leucine mutation reacts normally with the GTPase activating protein GAP but nevertheless has transforming properties. *J. Biol. Chem. 266*, 17700–17706.
55. Wu, W. J., Tu, S., and Cerione, R. A. (2003) Activated Cdc42 sequesters c-Cbl and prevents EGF receptor degradation. *Cell 114*, 715–725.
56. Saville, B. (1958) A scheme for the colorimetric determination of microgram amounts of thiols. *Analyst 83*, 670–672.
57. John, J., Sohmen, R., Feuerstein, J., Linke, R., Wittinghofer, A., and Goody, R. S. (1990) Kinetics of interaction of nucleotides with nucleotide-free H-ras p21. *Biochemistry 29*, 6058–6065.
58. Lenzen, C., Cool, R. H., and Wittinghofer, A. (1995) Analysis of intrinsic and CDC25-stimulated guanine nucleotide exchange of p21ras-nucleotide complexes by fluorescence measurements. *Methods Enzymol. 255*, 95–109.
59. Heo, J., and Holbrook, G. (1999) Regulation of 2-carboxy-D-arabinitol 1-phosphate phosphatase: activation by glutathione and interaction with thiol reagents. *Biochem. J. 338*, 409–416.
60. Butler, A. R., and Megson, I. L. (2002) Non-heme iron nitrosyls in biology. *Chem. Rev. 102*, 1155–1166.

61. Li, C., Teng, R. H., Tsai, Y. C., Ke, H. S., Huang, J. Y., Chen, C. C., Kao, Y. L., Kuo, C. C., Bell, W. R., and Shieh, B. (2005) H-Ras oncogene counteracts the growth-inhibitory effect of genistein in T24 bladder carcinoma cells. *Br. J. Cancer 92*, 80–88.
62. Rait, A., Pirollo, K., Will, D. W., Peyman, A., Rait, V., Uhlmann, E., and Chang, E. H. (2000) 3′-End conjugates of minimally phosphorothioate-protected oligonucleotides with 1-O-hexadecylglycerol: synthesis and anti-ras activity in radiation-resistant cells. *Bioconjugate Chem. 11*, 153–160.
63. Chen, G., Oh, S., Monia, B. P., and Stacey, D. W. (1996) Antisense oligonucleotides demonstrate a dominant role of c-Ki-RAS proteins in regulating the proliferation of diploid human fibroblasts. *J. Biol. Chem. 271*, 28259–28265.
64. Liu, H. S., Lin, C. N., and Won, S. J. (1997) Antitumor effect of 2,6-di(2,3-epoxypropoxy)xanthone on tumor cell lines. *Anticancer Res. 17*, 1107–1114.
65. Morgan, C. J., Chawdry, R. N., Smith, A. R., Siravo-Sagraves, G., and Trewyn, R. W. (1994) 6-Thioguanine-induced growth arrest in 6-mercaptopurine-resistant human leukemia cells. *Cancer Res. 54*, 5387–5393.
66. Kaba, S. E., Kyritsis, A. P., Hess, K., Yung, W. K., Mercier, R., Dakhil, S., Jaeckle, K. A., and Levin, V. A. (1997) TPDC-FuHu chemotherapy for the treatment of recurrent metastatic brain tumors. *J. Clin. Oncol. 15*, 1063–1070.
67. Bae, S. K., Baek, J. H., Lee, Y. M., Lee, O. H., and Kim, K. W. (1998) Hypoxia-induced apoptosis in human hepatocellular carcinoma cells: a possible involvement of the 6-TG-sensitive protein kinase(s)-dependent signaling pathway. *Cancer Lett. 126*, 97–104.
68. Matheson, E. C., and Hall, A. G. (1999) Expression of DNA mismatch repair proteins in acute lymphoblastic leukaemia and normal bone marrow. *Adv. Exp. Med. Biol. 457*, 579–583.
69. Liu, T., Raetz, E., Moos, P. J., Perkins, S. L., Bruggers, C. S., Smith, F., and Carroll, W. L. (2002) Diversity of the apoptotic response to chemotherapy in childhood leukemia. *Leukemia 16*, 223–232.
70. Cuffari, C., Seidman, E. G., Latour, S., and Theoret, Y. (1996) Quantitation of 6-thioguanine in peripheral blood leukocyte DNA in Crohn's disease patients on maintenance 6-mercaptopurine therapy. *Can. J. Physiol. Pharmacol. 74*, 580–585.
71. Teml, A., Schaeffeler, E., Herrlinger, K. R., Klotz, U., and Schwab, M. (2007) Thiopurine treatment in inflammatory bowel disease: clinical pharmacology and implication of pharmacogenetically guided dosing. *Clin. Pharmacokinet. 46*, 187–208.
72. Sahasranaman, S., Howard, D., and Roy, S. (2008) Clinical pharmacology and pharmacogenetics of thiopurines. *Eur. J. Clin. Pharmacol. 64*, 753–767.
73. Lander, H. M., Milbank, A. J., Tauras, J. M., Hajjar, D. P., Hempstead, B. L., Schwartz, G. D., Kraemer, R. T., Mirza, U. A., Chait, B. T., Burk, S. C., and Quilliam, L. A. (1996) Redox regulation of cell signalling. *Nature 381*, 380–381.
74. Raines, K. W., Cao, G. L., Lee, E. K., Rosen, G. M., and Shapiro, P. (2006) Neuronal nitric oxide synthase-induced S-nitrosylation of H-Ras inhibits calcium ionophore-mediated extracellular-signal-regulated kinase activity. *Biochem. J. 397*, 329–336.
75. Lenzen, C., Cool, R. H., Prinz, H., Kuhlmann, J., and Wittinghofer, A. (1998) Kinetic analysis by fluorescence of the interaction between Ras and the catalytic domain of the guanine nucleotide exchange factor $Cdc25^{Mm}$. *Biochemistry 37*, 7420–7430.
76. Pai, E. F., Kabsch, W., Krengel, U., Holmes, K. C., John, J., and Wittinghofer, A. (1989) Structure of the guanine-nucleotide-binding domain of the Ha-ras oncogene product p21 in the triphosphate conformation. *Nature 341*, 209–214.
77. Tong, L. A., de Vos, A. M., Milburn, M. V., Jancarik, J., Noguchi, S., Nishimura, S., Miura, K., Ohtsuka, E., and Kim, S. H. (1989) Structural differences between a ras oncogene protein and the normal protein. *Nature 337*, 90–93.
78. Pai, E. F., Krengel, U., Petsko, G. A., Goody, R. S., Kabsch, W., and Wittinghofer, A. (1990) Refined crystal structure of the triphosphate conformation of H-ras p21 at 1.35 A resolution: implications for the mechanism of GTP hydrolysis. *EMBO J. 9*, 2351–2359.
79. Plattner, R., Anderson, M. J., Sato, K. Y., Fasching, C. L., Der, C. J., and Stanbridge, E. J. (1996) Loss of oncogenic ras expression does not correlate with loss of tumorigenicity in human cells. *Proc. Natl. Acad. Sci. U.S.A. 93*, 6665–6670.
80. Gupta, S., Stuffrein, S., Plattner, R., Tencati, M., Gray, C., Whang, Y. E., and Stanbridge, E. J. (2001) Role of phosphoinositide 3-kinase in the aggressive tumor growth of HT1080 human fibrosarcoma cells. *Mol. Cell. Biol. 21*, 5846–5856.
81. Kraus, P., and Kloft, H. D. (1980) The activity of glutathione-S-transferases in various organs of the rat. *Enzyme 25*, 158–160.
82. Rahman, S. H., Ibrahim, K., Larvin, M., Kingsnorth, A., and McMahon, M. J. (2004) Association of antioxidant enzyme gene polymorphisms and glutathione status with severe acute pancreatitis. *Gastroenterology 126*, 1312–1322.
83. Eklund, B. I., Moberg, M., Bergquist, J., and Mannervik, B. (2006) Divergent activities of human glutathione transferases in the bioactivation of azathioprine. *Mol. Pharmacol. 70*, 747–754.
84. Deneke, S. M. (2000) Thiol-based antioxidants. *Curr. Top. Cell. Regul. 36*, 151–180.
85. Filomeni, G., Rotilio, G., and Ciriolo, M. R. (2002) Cell signalling and the glutathione redox system. *Biochem. Pharmacol. 64*, 1057–1064.
86. Lopez-Mirabal, H. R., and Winther, J. R. (2008) Redox characteristics of the eukaryotic cytosol. *Biochim. Biophys. Acta 1783*, 629–640.
87. Poole, L. B., and Nelson, K. J. (2008) Discovering mechanisms of signaling-mediated cysteine oxidation. *Curr. Opin. Chem. Biol. 12*, 18–24.
88. Kupan, A., Sauliere, A., Broussy, S., Seguy, C., Pratviel, G., and Meunier, B. (2006) Guanine oxidation by electron transfer: one-versus two-electron oxidation mechanism. *ChemBioChem 7*, 125–133.
89. Bonini, M. G., Miyamoto, S., Di Mascio, P., and Augusto, O. (2004) Production of the carbonate radical anion during xanthine oxidase turnover in the presence of bicarbonate. *J. Biol. Chem. 279*, 51836–51843.
90. Joffe, A., Mock, S., Yun, B. H., Kolbanovskiy, A., Geacintov, N. E., and Shafirovich, V. (2003) Oxidative generation of guanine radicals by carbonate radicals and their reactions with nitrogen dioxide to form site specific 5-guanidino-4-nitroimidazole lesions in oligodeoxynucleotides. *Chem. Res. Toxicol. 16*, 966–973.
91. Traut, T. W. (1994) Physiological concentrations of purines and pyrimidines. *Mol. Cell. Biochem. 140*, 1–22.
92. Warren, R. B., and Griffiths, C. E. (2005) The potential of pharmacogenetics in optimizing the use of methotrexate for psoriasis. *Br. J. Dermatol. 153*, 869–873.
93. Raines, K. W., Cao, G. L., Porsuphatana, S., Tsai, P., Rosen, G. M., and Shapiro, P. (2004) Nitric oxide inhibition of ERK1/2 activity in cells expressing neuronal nitric-oxide synthase. *J. Biol. Chem. 279*, 3933–3940.
94. Mizuno, S., Kadowaki, M., Demura, Y., Ameshima, S., Miyamori, I., and Ishizaki, T. (2004) p42/44 Mitogen-activated protein kinase regulated by p53 and nitric oxide in human pulmonary arterial smooth muscle cells. *Am. J. Respir. Cell Mol. Biol. 31*, 184–192.
95. Segel, I. H. (1993) Enzyme kinetics, Wiley-Interscience, New York.